Real-Time Adaptively Regularized Compressive Sensing in Cognitive Radio Networks

Xingjian Zhang, *Student Member, IEEE*, Yuan Ma, *Member, IEEE*, Yue Gao, *Senior Member, IEEE*, and Shuguang Cui, *Fellow, IEEE*

***Abstract*—Wideband spectrum sensing is regarded as one of the key functional blocks in cognitive radio systems, where compressive sensing (CS) has become one of the promising techniques to deal with the Nyquist sampling rate bottleneck. Theoretical analyses and simulations have shown that CS could achieve both high detection and low false alarm probabilities in wideband spectrum sensing. However, the implementation of CS over real-world signals and real-time processing poses significant challenges due to the high computational burden and reconstruction errors against noise. In this paper, we propose an efficient adaptively regularized iterative reweighted least squares (AR-IRLS) algorithm to implement the real-time signal recovery in CS-based wideband spectrum sensing. The proposed AR-IRLS algorithm moves the estimated solutions along an exponential–linear path by regularizing weights with a series of nonincreasing penalty terms, which significantly speeds up the convergence of reconstruction and provides a high fidelity guarantee to cope with spectral signals with varying bandwidths and power levels. Furthermore, a descent-based decision threshold setting algorithm is proposed to distinguish the primary signals from the mixture of the reconstruction errors and unknown noises. The proposed scheme demonstrates robustness against different sparsity levels at low compressive ratios without degradation of the reconstruction performance. It is tested with the real-world signals over the TV white space after being validated with the simulated signals. Both the simulation and real-time experiments show that the proposed scheme outperforms the conventional iterative reweighted least squares algorithms in terms of convergence speed, reconstruction accuracy, and compressive ratio.**

***Index Terms*—Cognitive radio, compressive wideband spectrum sensing, iterative reweighted least squares (IRLS), l_v-norm minimization, TV white space.**

Manuscript received January 23, 2017; revised June 1, 2017; accepted August 6, 2017. Date of publication September 28, 2017; date of current version February 12, 2018. This work was supported in part by the Engineering and Physical Sciences Research Council (EPSRC) in the U.K. under Grant EP/L024241/1, in part by the DoD under Grant HDTRA1-13-1-0029, in part by the National Natural Science Foundation of China under Grant 61328102/61629101, and in part by the National Natural Science Foundation under Grant DMS-1622433, Grant AST-1547436, Grant ECCS-1508051/1659025, and Grant CNS-1343155. The review of this paper was coordinated by Prof. S. Zhang. *(Corresponding author: Y. Ma.)*

X. Zhang, Y. Ma, and Y. Gao are with the School of Electronic Engineering and Computer Science, Queen Mary University of London, London E1 4NS, U.K. (e-mail: xingjian.zhang@qmul.ac.uk; y.ma@qmul.ac.uk; yue.gao@ieee.org).

S. Cui is with the Department of Electrical and Computer Engineering, University of California, Davis, CA 95616 USA. He is also with Beijing Advanced Innovation Center for Future Internet Technology, Beijing 100124, China (e-mail: sgcui@ucdavis.edu).

Color versions of one or more of the figures in this paper are available online at http://ieeexplore.ieee.org.

Digital Object Identifier 10.1109/TVT.2017.2749254

I. Introduction

With the rapid development of wireless communication, the current static frequency allocation policy faces a primary challenge of spectrum scarcity, while a significant portion of the spectrum resource remains underutilized in the temporal and spatial dimensions [1], [2]. Cognitive radio (CR) has been considered as one of the promising solutions to tackle the spectrum scarcity in future wireless networks, i.e., 5G and beyond. In most locations around the world, there is certain unused TV band spectrum, named as TV white space (TVWS), which could be used for a range of wireless applications, from broadband communication, wireless offloading, to machine-to-machine communication [3]. Unlocking the TVWS spectrum implies significantly increasing the total amount of bandwidth available for users, therefore alleviating the pressure on other spectrum bands [4].

To put such unused ultra high frequency (UHF) TV spectrum to good usages, we need fast and reliable occupancy detection of the surrounding spectrum such that no interferences are caused to the transmissions of primary users (PUs). Currently, there mainly exist two approaches to obtain the spectrum occupancy status over TVWS. One is through a geo-location database that calculates the interference generated in wireless communication systems through theoretical propagation models and then outputs the maximum allowable equivalent isotropic radiated power (EIRP) for each vacant TVWS channel at a specific location and time [5]. However, the geo-location database only records the information of the licensed PUs. Consequently, unpredictable dynamic changes of the wireless propagation environment could pose significant challenges to this approach. To that end, dynamic spectrum sensing in CR is introduced to tackle these challenges [6], [7].

Spectrum sensing is defined as the task of finding spectrum holes over time and space domain by the secondary users (SUs) in an unsupervised manner. Nevertheless, the wide spectrum of TVWS challenges the traditional spectrum sensing schemes in terms of the sampling rate, computational complexity, and real-time processing [8]. Exploiting the sparse nature of the underutilized wideband spectrum, sparse representation techniques have shown huge potential capabilities in handling these problems, which are directly related to compressive sensing (CS) from the viewpoint of its origin [9], [10]. CS theory indicates that if a signal has the sparse structure, i.e., the intra-signal correlation, that signal can be reconstructed by exploiting a

few samples, which are much less than the ones suggested by previously used theories such as Nyquist-Shannon's sampling theorem. The entire process of CS consists of three parts: signal sparse representation; measurement collection (linear encoding); sparse reconstruction (nonlinear decoding). Apart from the intra-signal correlation, signals from multiple sensors in a network may have the high spatial correlation which represents inter-signal correlation [11]. Recently, sparse Bayesian learning based distributed CS algorithms are proposed in [11], [12] for joint reconstruction of multiple signals to leverage inter-signal correlation. These algorithms are able to achieve superior performance by utilizing the networked sensing systems. In this work, we concentrate on the real-time processing in the single node.

To overcome the Nyquist sampling rate bottleneck and reduce computational complexity, several new compressive sampling methods have been proposed [13]–[18], where the sampling rate could be reduced by exploiting some specific features of the spectrum. In [13], a compressive spectrum sensing approach over wide spectrum was proposed by utilizing the embedded sparsity of the edge spectrum. In [14], [15], power spectrum estimation over the compressive samples has been proposed by concentrating on the autocorrelation of the compressive samples instead of the original signal itself. In [16]–[19], sub-Nyquist sampling approaches have been developed based on multicoset sampling to estimate the spectrum by recovering the frequency support of the multiband signals. Although these algorithms can reduce the sampling requirement and computational complexity, they depend on prior spectral assumptions such as fixed channel bandwidth and power levels and concentrate on the partial signal reconstruction.

In recent years, as the secondary spectrum market has been opened for spectrum sharing, an increasing number of programme making and special event (PMSE) users are joining for public access, which cover a wide range of radio systems, e.g., wireless microphones, continuous talkback systems, high-quality audio links, remote controllers, etc [20]. As PMSE users have varying channel bandwidths and radiated levels (up to 200 kHz and 10 mW respectively), accurate detection of the PMSE users and other PUs with varying power levels challenges the traditional compressive spectrum sensing algorithms [13]–[15]. Therefore, the full reconstruction of the wideband signals with the high fidelity guarantee is of critical importance to work with real-world signals in achieving reliable spectrum detection.

To find the optimal solution that best matches the compressive projections, the original wideband signals can be reconstructed using certain optimization strategies based on l_0-norm minimization [21]. Since l_0-norm minimization is an NP-hard problem, l_1-norm minimization is usually utilized to find an equivalent solution based on the restricted isometry property (RIP) [22]. To further improve the recovery performance with less requirements on the signal sparsity and the number of compressive samples, the weighted l_ν-norm ($0 < \nu < 1$) minimization is proposed to replace the l_1-norm minimization, which is nonconvex but could be solved by iteratively reweighted least squares (IRLS) algorithm [23]. As the l_ν-norm minimization provides a closer approximation to the l_0-norm minimization, the weighted l_ν-norm minimization is a more efficient solution to exactly reconstruct the original signals [24]–[27]. However, without any prior information on the original signals, conventional IRLS algorithms could lead to relatively high computational complexity and need to run through many iterations to achieve the desired signal recovery, which incurs a large latency and is difficult to be implemented in real-time processing [24].

In addition, the performance of spectrum sensing greatly depends on the detection methods over the reconstructed signal. Energy detection is the most widely used detection method since it is simple, to implement and does not require any prior information about the spectral, features of primary signals [28], [29]. Most conventional energy detection algorithms adopt a fixed or adaptive decision threshold to distinguish PU signals from the noise [30], which is calculated via prior knowledge over the noise power. However, it is difficult to guarantee the detection and false alarm probabilities with the traditional threshold setting algorithms when the noise power is unknown or fluctuates in real-time wideband spectrum sensing. In [31], the decision threshold setting is based on the noise power measured in the vacant channels. However, it is difficult to distinguish which channels contain noise only without related prior information in practice. Moreover, the power level of noise is likely to change after the reconstruction process [32]. Besides, we notice that most of the existing compressive wideband spectrum sensing schemes do not specify the reconstruction errors from the compressive samples, which inevitably exists and interferes the detection. Therefore, a practical and effective reconstruction strategy that can dynamically eliminates the influence of CS reconstruction errors and distorted noise floors is critical to enable accurate real-time wideband spectrum sensing.

In this paper, an adaptively-regularized CS scheme is proposed to implement the real-time wideband spectrum sensing. The proposed AR-IRLS algorithm moves the estimated solutions along an exponential-linear path by regularizing weights with a series of nonincreasing penalty terms, which significantly speeds up the convergence of the signal reconstruction by reducing the required iterations (up to 70%) and provides high fidelity guarantees to cope with the varying bandwidths and power levels over the occupied channels. Moreover, to eliminate the impact of noise uncertainty and reconstruction errors, a practical descent-based algorithm for decision threshold setting is proposed. Based on our recent work on the trials over TVWS [4], [33], the proposed scheme is further tested to support the implementation of real-time dynamic spectrum access over the TVWS. From the evaluation of the reconstruction performance, it is shown that the proposed AR-IRLS algorithm is able to deal with real-world signals in real-time wideband spectrum sensing, with improvements over the convergence speed as well as sensing cost when compared with conventional iterative l_ν-norm minimization approaches.

The rest of the paper is organized as follows. In Section II, the preliminary system model is described. Section III introduces the proposed AR-IRLS algorithm. Section IV develops the proposed descent-based algorithm for decision threshold setting. Section V analyzes and validates the proposed algorithms over

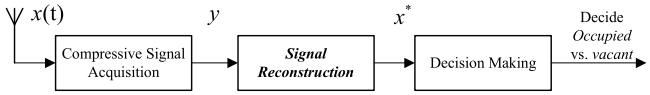

Fig. 1. Block diagram of CS-based wideband spectrum sensing scheme.

simulated and real-world TVWS signals for real-time processing. Conclusions are drawn in Section VI.

II. Preliminary System Model

A typical CS-based wideband spectrum sensing scheme can be presented as a three-step framework, as shown in Fig. 1.

1) Compressive signal acquisition: The basic idea of CR is spectrum sharing, which allows the unlicensed users, i.e., SUs, to communicate over licensed spectrum when the bands are not fully utilized by PUs. The received signal $x(t)$ at the CR is usually assumed to be bandlimited and continuous, which consists of N_{sig} uncorrelated primary signals in addition to the noise. The primary signals are superposed in the time domain but occupied the different region of the spectrum, such that

$$x(t) = \sum_{i=1}^{N_{\text{sig}}} s_i(t) + n(t), \tag{1}$$

where $s_i(t)$ is the i-th primary signal and $n(t)$ refers to additive white Gaussian noise with zero mean and variance σ_n^2. Since the wideband spectrum is practically underutilized [34], $x(t)$ typically bears a sparse property in the frequency domain such that its discrete Fourier transform $\boldsymbol{x} \in \mathbb{R}^N$ is a k-sparse vector, i.e., $|\{x_i : x_i \neq 0\}| \leq k$. The compressive samples acquisition at each SU can be expressed by the following analytical model:

$$\boldsymbol{y} = \boldsymbol{\Phi x} \quad \text{subject to } ||\boldsymbol{x}||_0 \leq k, \tag{2}$$

where $\boldsymbol{\Phi} \in \mathbb{R}^{M \times N}$ is the sensing matrix to generate the compressive samples $\boldsymbol{y} \in \mathbb{R}^M$ from the original signal, $M \in \mathbb{Z}$ (with $k < M < N$) refers to the dimension of $\boldsymbol{y}$ and $||\cdot||_0$ represents the number of nonzero elements in the vector, which is also treated as the measure of sparsity.

It turns out that the real-world sampling always leads to noise. Thus, (2) could be modified to a revised model incorporating the small noise perturbation as

$$\boldsymbol{y} = \boldsymbol{\Phi x} + \boldsymbol{\xi} \quad \text{subject to } ||\boldsymbol{x}||_0 \leq k, \tag{3}$$

where $\boldsymbol{\xi} \in \mathbb{R}^M$ is the noise perturbation, whose magnitude is constrained by an upper bound δ, i.e., $||\boldsymbol{\xi}||_2 < \delta$. Incidentally, the compressive ratio in this sub-Nyquist signal acquisition is given by $\rho = M/N < 1$.

2) Signal reconstruction: Under certain assumptions including the RIP on $\boldsymbol{\Phi}$ and the signal sparsity bound [22], robust signal reconstruction with respect to model (3) at each SU can be achieved as

$$\arg\min_{\boldsymbol{x} \in \mathbb{R}^N} ||\boldsymbol{x}||_0 \quad \text{subject to } ||\boldsymbol{\Phi x} - \boldsymbol{y}||_2^2 \leq \delta, \tag{4}$$

which aims to seek a maximally sparse representation of $\boldsymbol{y}$, or

$$\arg\min_{\boldsymbol{x} \in \mathbb{R}^N} ||\boldsymbol{\Phi x} - \boldsymbol{y}||_2^2 \quad \text{subject to } ||\boldsymbol{x}||_0 \leq k, \tag{5}$$

which finds the possible minimum reconstruction error at a given sparsity k. In practice, the original signals tend to be compressible, rather than sparse, where a compressible signal has a representation whose entries decay rapidly when sorted in the decreasing order of magnitude. Although compressible signals can be well approximated by sparse signals, the reconstruction errors can only be diminished but not vanished [21]. Therefore, according to the Lagrange multiplier theorem, a proper constant parameter $\lambda > 0$ could be introduced to balance the objective of minimizing the reconstruction error and the solution sparsity, such that problems (4) and (5) could be equivalently solved by solving the following unconstrained minimization problem:

$$\arg\min_{\boldsymbol{x} \in \mathbb{R}^N} \frac{1}{2} ||\boldsymbol{\Phi x} - \boldsymbol{y}||_2^2 + \lambda ||\boldsymbol{x}||_0. \tag{6}$$

However, problems (4), (5) and (6) are known to be NP-hard in general, which cannot be solved efficiently. It was shown in [35], [36] that the solution via the l_1-norm minimization with sufficient sparsity can be equivalent to the solution obtained by the l_0-norm minimization, where the l_1-norm optimization problem can be solved in polynomial time. Thus, problems (4), (5) and (6) can be efficiently and approximately solved by solving the following problems:

$$\arg\min_{\boldsymbol{x} \in \mathbb{R}^N} ||\boldsymbol{x}||_1 \quad \text{subject to } ||\boldsymbol{\Phi x} - \boldsymbol{y}||_2^2 \leq \delta, \tag{7}$$

or equivalently,

$$\arg\min_{\boldsymbol{x} \in \mathbb{R}^N} \frac{1}{2} ||\boldsymbol{\Phi x} - \boldsymbol{y}||_2^2 + \lambda ||\boldsymbol{x}||_1. \tag{8}$$

Since $||\boldsymbol{\Phi x} - \boldsymbol{y}||_2^2$ is a convex quadratic function, (8) is shown to be efficient under certain conditions in finding a sparse representation to achieve a small $||\boldsymbol{\Phi x} - \boldsymbol{y}||_2^2$ [37]; but it may not be the optimal solution to problem (6) since the l_1-norm optimization problem usually requires much more compressive samples [24]. Therefore, this poses challenges when the signal dimension is high, i.e., when we have wideband spectrum signals. Thus, we propose to replace the l_1-norm in (8) with the l_v-norm, for $0 < v < 1$, which is possible to achieve the exact reconstruction with substantially fewer samples [24], [26].

3) Decision making: When the recovered signal $\boldsymbol{x^*}$ is obtained by solving the optimization problem discussed above, energy detection could be applied to determine the spectrum occupancy by comparing the energy density of the recovered signal against a predefined threshold φ_d, which for example could be set as [38]

$$\varphi_d = \sigma_n^2 \left(1 + \frac{Q^{-1}(P_f)}{\sqrt{N/2}}\right), \tag{9}$$

where σ_n^2 is the noise variance and P_f refers to the target probability of false alarm. If the energy of the reconstructed signal is higher than the threshold, the corresponding channel is determined as occupied by PU, and SUs are forbidden to access. Otherwise, the corresponding channel is determined as vacant, and SUs could access to transmit unlicensed signals. It should be noted that the detection performance would benefit from higher CS reconstruction accuracy. Indicated by (9), the performance of energy detection greatly depends on setting the detection

threshold, which is mainly decided by the noise variance and the target probability of false alarm. However, most traditional wideband spectrum sensing schemes, which assume the noise variance as a prior knowledge, are no longer suitable for real-time wideband spectrum sensing where the noise variance is unknown and likely varying. To tackle this issue, a practical descent-based decision threshold setting algorithm for eliminating the impact of noise and reconstruction errors without the prior knowledge of the noise floor is proposed in Section IV.

III. Proposed Adaptively-Regularized IRLS Algorithm

In this section, we seek a better solution for the problem in (6) by the l_ν-norm approximation. The description of the proposed algorithm is sketched first and then we provide some theoretical guarantees.

A. Algorithm Description

The basic idea of the proposed algorithm is to find a surrogate function based on the l_ν-norm to majorize the objective function in (6), and then to minimize the surrogate function to drive the objective function downward until a global optimum is reached. In particular, we conduct the relaxation of the l_0-norm problem by utilizing the l_ν-norm instead of the l_1-norm in (8). In contrast to the l_1-norm, the l_ν-norm with $0 < \nu < 1$ is nonconvex. As convex optimization techniques are no longer applicable, the l_ν-norm makes the solution uniqueness and convergence analysis more complicated. However, fewer samples are usually required for the l_ν-norm approach compared with the l_1-norm approach [24]. Moreover, it was shown in [24], [39] that the l_ν-norm regularization leads to better sparsity approximation performance than l_1-norm. This is because l_ν-norm not only enforces stronger sparsity than l_1-norm, but it also better preserves edges [40], which is capable of yielding a sparser solution with higher fidelity than the l_1-norm regularization.

Given a function f that is convex, the l_ν-norm regularized problem can be presented as

$$\arg\min_{\boldsymbol{x}\in\mathbb{R}^N} \; f(\boldsymbol{x}) + \lambda ||\boldsymbol{x}||_\nu^\nu \quad 0 < \nu < 1. \tag{10}$$

As $||\boldsymbol{\Phi x} - \boldsymbol{y}||_2^2$ is a convex quadratic function and therefore a valid choice for f in (10), we can transform (6) into the following unconstrained regularization problem:

$$\arg\min_{\boldsymbol{x}\in\mathbb{R}^N} \frac{1}{2}||\boldsymbol{\Phi x} - \boldsymbol{y}||_2^2 + \lambda ||\boldsymbol{x}||_\nu^\nu \quad 0 < \nu < 1. \tag{11}$$

Since problem (11) is intermediate in the sense of norm minimization between problems (6) and (8), one can expect that it is also capable of seeking out a solution to (6) under certain conditions. Here, as discussed before, $\lambda > 0$ is the penalty parameter that balances the reconstruction accuracy and the sparsity of the minimization result. In addition, the choice of λ depends on the noise level of the original signal, e.g., the value of λ should be increased when the noise is larger [41]. Therefore, for the varying wideband spectrum signal in a real-time processing environment, the choice of λ greatly influences the behavior of the spectrum reconstruction, such that we need to find the most suitable value of λ for difference signals. Some approaches have been proposed for determining λ. However, these approaches are based on some extra algorithms [42], [43], which leads to increased computational complexity. In our work, we optimize λ along with the signal reconstruction process and λ is defined as a function of the target signal such that the problem in (11) can be transformed into the following form:

$$\arg\min_{\boldsymbol{x}\in\mathbb{R}^N} \{F(\boldsymbol{x}) = \frac{1}{2}||\boldsymbol{\Phi x} - \boldsymbol{y}||_2^2 + \lambda(\boldsymbol{x})||\boldsymbol{x}||_\nu^\nu\} \quad 0 < \nu < 1, \tag{12}$$

where $\lambda(\boldsymbol{x})$ projects the signal $\boldsymbol{x}$ as a positive real number. In order to retain the numerical property of the original problem, $\lambda(\boldsymbol{x})$ should be a function of the smoothing functional, e.g., we could set it in general as $\lambda(\boldsymbol{x}) = g(F(x))$, where $g(\cdot)$ is a monotonically increasing function. Moreover, the objective function in each iteration should preserve its convexity and exhibits only a global minimizer regardless of the value of $\lambda(\boldsymbol{x})$. Therefore, we utilize the linear function of the form: $F(x) = \varrho\lambda(\boldsymbol{x})$ [44], where ϱ is the coefficient representing the slope of the line and also controls convexity. It is straightforward to show that this linear form could keep the numerical property of the original problem unchanged. Therefore, from (12), $\lambda(\boldsymbol{x})$ can be expressed as

$$\lambda(\boldsymbol{x}) = \frac{\frac{1}{2}||\boldsymbol{\Phi x} - \boldsymbol{y}||_2^2}{\varrho - ||\boldsymbol{x}||_\nu^\nu} \quad 0 < \nu < 1 \tag{13}$$

However, it is general computationally hard and not guaranteed to obtain its global minimum due to the nonconvexity of the l_ν-norm. An alternative approach is to solve a sequence of the approximation subproblems, named as IRLS [23], [24], [26]. It is shown in [24] that under certain assumptions such as the null space property (NSP) on $\boldsymbol{\Phi}$, the solution sequence generated by the IRLS algorithm converges to the local minimum as the sparsest solution that is also the actual global l_ν-norm minimizer. Therefore, this IRLS method could be utilized to solve the unconstrained l_ν-norm minimization problem in (12).

In particular, each iteration of the IRLS algorithm corresponds to a weighted least squares subproblem that can be efficiently solved by standard convex optimization methods. Let the weight $\boldsymbol{w} \in \mathbb{R}^N$ be a vector with each element being a positive number, i.e., $w_i > 0$ for all $i = 1, 2, ..., N$. The corresponding weighted inner product and weighted l_2-norm, are defined as

$$\begin{aligned} \langle \boldsymbol{a}, \boldsymbol{b}\rangle_{\boldsymbol{w}} &:= \sum_{i=1}^{N} w_i a_i b_i \\ ||\boldsymbol{a}||_2^{2(\boldsymbol{w})} &:= \langle \boldsymbol{a}, \boldsymbol{a}\rangle_{\boldsymbol{w}}. \end{aligned} \tag{14}$$

Without knowing apriori the spectral support of the original signal, the procedure for selecting weights is iterative in nature. A typical approach updates the weights at each iteration by using the solution of the weighted least squares problem from the previous iteration, i.e., $\boldsymbol{w}^{(l)} := |\boldsymbol{x}^{(l-1)}|^{-1}$ [23]. Specifically, the IRLS algorithm generates a sequence $\{\boldsymbol{x}^{(l)}\}_{l=1}^{\infty}$ which are the

iterative estimates of $\boldsymbol{x}$ and given by

$$\begin{aligned}\boldsymbol{x}^{(l)} &:= \arg\min_{\boldsymbol{x}\in\mathcal{J}(\boldsymbol{x})} \frac{1}{2}||\boldsymbol{\Phi x}-\boldsymbol{y}||_2^2 + \lambda(\boldsymbol{x}^{(l-1)})||\boldsymbol{x}||_2^{2(\boldsymbol{w}^{(l)})},\\ \boldsymbol{w}^{(l)} &:= (w_1^{(l)}, ..., w_N^{(l)}),\end{aligned} \tag{15}$$

where $w_j^{(l)} := |x_j^{(l-1)}|^{-1}$, and the set $\mathcal{J}(\boldsymbol{x}) = \{\boldsymbol{x} \mid ||\boldsymbol{\Phi x}-\boldsymbol{y}||_2^2 \le \delta\}$ represents the set of feasible points to (4). Therefore, the weighted least squares problem in each iteration of the IRLS algorithm works over a closed convex set $\mathcal{J}(\boldsymbol{x})$, and can be efficiently solved using standard convex optimization methods.

However, if one of the elements $x_j^{(l)}$ vanishes at some iteration l, i.e., $x_j^{(l)} \to 0$, the corresponding weight component $w_j^{(l+1)} \to \infty$, which leads to $x_j^{(l+1)} = 0$ at the next iteration as well and persists in all sequential iterations, resulting in certain loss of information. As such, a small fixed regularizer $\epsilon > 0$ [26] could be adopted to regularize the optimization problem in order to provide stability and ensure that a zero-valued component in $\boldsymbol{x}^{(l)}$ does not strictly prohibit a nonzero estimate at the next iteration, as shown below:

$$w_i^{(l)} = \left(\left(x_i^{(l-1)}\right)^2 + \epsilon\right)^{\frac{\nu}{2}-1} \quad 0 < \nu < 1. \tag{16}$$

Following the arguments in [27], the l_ν-norm ($0 < \nu < 1$) could closely approximate the l_0-norm by setting a small enough ϵ, where a large fixed ϵ leads to inaccurate results. Unfortunately, as $\epsilon \to 0$, the regularizing functionality of ϵ becomes weak. That would cause the loss of certain information during the optimization as we discussed before. Thus, fixing ϵ relatively small or high would not be an optimal choice. A scheme where ϵ is dynamically decreased in each step is suggested in [23], which is based on the knowledge over anticipated accuracy for arbitrary signal recovery. Although this approach provides the l_ν-norm with a better l_0-norm approximation, ϵ would get to zero and some of the weights would be infinite since the reconstructed signals in some iterations could be sparser than the original signal. Therefore, it does not offer theoretical guarantees and would lead to some wrong local solutions.

To speed up the convergence and prevent getting trapped into the wrong local solutions, we propose to start with a relatively large regularizer which is given as Ω_ϵ for $\boldsymbol{w}^{(0)}$, and then quickly update the weights at each iteration by exponentially decreasing Ω_ϵ in the first few iterations, as a smaller regularizer allows the optimization process go deeper to achieve higher reconstruction accuracy [45]. We then let Ω_ϵ descend slowly in order to prevent $\Omega_\epsilon \to 0$ while keeping Ω_ϵ sufficiently small. Finally the decrement of Ω_ϵ tends to be 0 when the iterations move towards the end. As the result of regularizing weights by the proposed algorithm, the estimated solutions is moved along an exponential-linear path. Even early iterations may get inaccurate reconstruction results, the primary elements in signal would be likely identified as nonzero values, such that their influences are diminished to provide chances for the algorithm to locate the remaining small but nonzero signal elements in later iterations.

Algorithm 1: Adaptively-regularized iterative reweighted least squares.

Require: samples vector $\boldsymbol{y} \in \mathbb{R}^N$, sensing matrix $\boldsymbol{\Phi} \in \mathbb{R}^{M\times N}$, $\Omega_\epsilon^{(0)} = 1$, $\boldsymbol{w^{(0)}} = 1, \ldots, 1$.
Ensure: Practical solution $\boldsymbol{x^*}$
1: **for** $l = 0, 1, \cdots, l_{\max}$ **do**
2: Constrained weighted least square minimization:

$$\boldsymbol{x^{(l)}} := \arg\min\ \Gamma_\nu(\boldsymbol{x^{(l-1)}}, \boldsymbol{w^{(l)}}, \Omega_\epsilon^{(l)})$$

3: Weights update: $\boldsymbol{w^{(l+1)}} = O(\boldsymbol{x^{(l)}}, \Omega_\epsilon^{(l)})$
4: Penalty parameter update:

$$\lambda(\boldsymbol{x^{(l)}}) = \frac{\frac{1}{2}||\boldsymbol{\Phi x^{(l)}}-\boldsymbol{y}||_2^2}{\varrho - \sum_{i=1}^N w_i^{(l+1)}(x_i^{(l)})^2}$$

5: Regularizer update:
6: **if** $||\Delta \boldsymbol{x^{(l)}}|| \le \frac{\epsilon^\nu}{100}$

$$\Omega_\epsilon^{(l+1)} = \left(1 + \frac{e^{-2l}}{h(\boldsymbol{x^{(l)}})_{s+1}}\right) h(\boldsymbol{x^{(l)}})_{s+1}$$

7: **else**
8: $\Omega_\epsilon^{(l+1)} = \Omega_\epsilon^{(l)}$
9: **end for**
10: **return** $\boldsymbol{x^*} = \boldsymbol{x^{(l+1)}}$;

To illustrate how the proposed algorithm works, a generalizing function Γ_ν is defined as

$$\Gamma_\nu(\boldsymbol{x}, \boldsymbol{w}, \Omega_\epsilon) := \left[\frac{1}{2}||\boldsymbol{\Phi x}-\boldsymbol{y}||_2^2 + \lambda(\boldsymbol{x})\sum_{i=1}^N w_i x_i^2\right], \tag{17}$$

where $\boldsymbol{x} \in \mathbb{R}^N$, $\boldsymbol{w} \in \mathbb{R}_+^N$, and $\Omega_\epsilon \in \mathbb{R}_+$. We initialize the parameters by setting $\boldsymbol{w^0} = 1, \ldots, 1$ and $\Omega_\epsilon^{(0)} = 1$. Therefore, (15) is equal to

$$\boldsymbol{x^{(l)}} := \arg\min\ \Gamma_\nu(\boldsymbol{x^{(l-1)}}, \boldsymbol{w^{(l)}}, \Omega_\epsilon^{(l)}), \tag{18}$$

which requires solving a weighted least squares problem that can be expressed in the matrix form:

$$\boldsymbol{x^{(l)}} = \boldsymbol{W^{(l)}\Phi^t}\left(\boldsymbol{\Phi W^{(l)}\Phi^t} + \lambda(\boldsymbol{x^{(l-1)}}) * \boldsymbol{I}\right)^{-1}\boldsymbol{y}, \tag{19}$$

where $\boldsymbol{W^{(l)}}$ is the $N \times N$ diagonal matrix with $1/w_i^{(l)}$ as the i-th diagonal element and $\boldsymbol{\Phi^t}$ refers to the transpose of the sensing matrix $\boldsymbol{\Phi}$. Once $\boldsymbol{x^{(l)}}$ is obtained, we then update the parameters as

$$\begin{aligned} w_j^{(l+1)} &:= O(\boldsymbol{x^{(l)}}, \Omega_\epsilon^{(l)}) = \left((x_j^{(l)})^2 + \Omega_\epsilon^{(l)}\right)^{\frac{\nu}{2}-1},\\ &\quad j = 1, ..., N,\\ \Omega_\epsilon^{(l+1)} &:= \begin{cases}\left(1 + \frac{e^{-2l}}{h(\boldsymbol{x^{(l+1)}})_{k+1}}\right) h(\boldsymbol{x^{(l)}})_{k+1}, & \text{if } ||\Delta \boldsymbol{x^{(l)}}|| \le \frac{\epsilon^\nu}{100}\\ \Omega_\epsilon^{(l)}, & \text{otherwise,}\end{cases}\end{aligned} \tag{20}$$

where $h(\boldsymbol{x})_i$ is the i-th largest element of the set $\{|\boldsymbol{x}|_j, j = 1, ..., N\}$, k refers to the sparsity of the signal, and $\Delta \boldsymbol{x^{(l)}} =$

$\boldsymbol{x}^{(l)} - \boldsymbol{x}^{(l-1)}$. From (17), we have

$$\lambda(\boldsymbol{x}) := \frac{\Gamma_\nu(\boldsymbol{x}, \boldsymbol{w}, \Omega_\epsilon) - \frac{1}{2}||\boldsymbol{\Phi x} - \boldsymbol{y}||_2^2}{\sum_{i=1}^N w_i x_i^2}. \tag{21}$$

We then substitute $\Gamma_\nu(\boldsymbol{x}, \boldsymbol{w}, \Omega_\epsilon) = \varrho \cdot \lambda(\boldsymbol{x})$ into (21), and obtain

$$\lambda(\boldsymbol{x}) = \frac{\frac{1}{2}||\boldsymbol{\Phi x} - \boldsymbol{y}||_2^2}{\varrho - \sum_{i=1}^N w_i x_i^2}. \tag{22}$$

In each iteration, to guarantee that the convexity of the function $\Gamma_\nu(\boldsymbol{x}, \boldsymbol{w}, \Omega_\epsilon)$ is unchanged, the penalty parameter should smaller than 1, i.e., $\lambda(\boldsymbol{x}) < 1$ [46]. From the convexity perspective, we have $\varrho > 1/2||\boldsymbol{\Phi x} - \boldsymbol{y}||_2^2 + ||\boldsymbol{x}||_2^{2(\boldsymbol{w})}$ by substituting $\lambda(\boldsymbol{x}) < 1$ into (22). Since $||\boldsymbol{x}||_2^{2(\boldsymbol{w})}$ could be approximated by $||\boldsymbol{x}||_2^\nu$ and $||\boldsymbol{x}||_2^\nu \simeq ||\boldsymbol{y}||_2^\nu$ according to [44] and

$$\frac{1}{2}||\boldsymbol{\Phi x} - \boldsymbol{y}||_2^2 = ||\boldsymbol{\xi}||_2^2 \le ||\boldsymbol{y}||_2^2, \tag{23}$$

where $||\boldsymbol{y}||_2^2 = ||\boldsymbol{\Phi x} + \boldsymbol{\xi}||_2^2$, the constraint $\lambda(\boldsymbol{x}) < 1$ could be obtained by setting $\varrho \ge \frac{1}{2}||\boldsymbol{y}||_2^2 + ||\boldsymbol{y}||_2^\nu$. Therefore, the value of control parameter ϱ is determined by the proposed algorithm according to the samples vector $\boldsymbol{y}$ in practice.

This whole process of reconstruction terminates when it converges or l reaches a specified maximum number of allowed iterations $l_{\max}$. The outline of the proposed algorithm is summarized in Algorithm 1.

B. Theoretical Guarantees

Theorem 1: (Null Space Property) From [23], we shall say that the matrix $\boldsymbol{\Phi}$ has the ν-Null Space Property (ν-NSP) of order S for $\gamma > 0$ if

$$||\eta_T||_\nu^\nu \le \gamma ||\eta_{T^c}||_\nu^\nu \tag{24}$$

for all sets T of cardinality not exceeding L and all $\eta \in \mathcal{N}$, where $\mathcal{N}$ is the null space of Φ as we defined before and T^c denotes the complement of the set T. In addition, η_T is the vector obtained from η by setting all coordinates $\eta_i = 0$ for $i \ne T \subset \{1, 2, \ldots, N\}$.

It is stated in [24] that in order to guarantee that a k-sparse vector $\boldsymbol{x}^*$ is the unique l_ν-norm minimizer of $\mathcal{J}(\boldsymbol{x})$, it is sufficient that $\boldsymbol{\Phi}$ has the ν-NSP ($0 < \nu < 1$) of order $s \le S$ with $\gamma \in (0, 1)$. Thus, we can extend this result to our weighted l_ν-norm minimization in (15).

1) Convergence: Theorem 1 ensures that, under certain conditions, the proposed algorithm has a unique exact solution according to [23], as established by the following theorem.

Theorem 2: Fix $\boldsymbol{y} \in \mathbb{R}^M$, define $\Gamma_\nu^n = \Gamma_\nu(\boldsymbol{x^n}, \boldsymbol{w^n}, \Omega_\epsilon^n)$ and let S be chosen such that $\boldsymbol{\Phi}$ satisfies the ν-NSP of order K. Then the sequence $\{\Gamma_\nu^n\}_{n=1}^\infty$ converges to a fixed point of the algorithm.

Proof: We first show that the sequence $\{\Gamma_\nu^n\}_{n=1}^\infty$ decreases monotonically over n, as we have the following monotonicity property hold for all $n \ge 0$:

$$\begin{aligned}\Gamma_\nu(\boldsymbol{x^{n+1}}, \boldsymbol{w^{n+1}}, \Omega_\epsilon^{n+1}) &\le \Gamma_\nu(\boldsymbol{x^{n+1}}, \boldsymbol{w^n}, \Omega_\epsilon^{n+1}) \\ &\le \Gamma_\nu(\boldsymbol{x^{n+1}}, \boldsymbol{w^n}, \Omega_\epsilon^n) \le \Gamma_\nu(\boldsymbol{x^n}, \boldsymbol{w^n}, \Omega_\epsilon^n).\end{aligned} \tag{25}$$

Here, the first inequality follows from the minimization property that defines $\boldsymbol{w^{n+1}}$, the second inequality from $\Omega_\epsilon^{n+1} \le \Omega_\epsilon^n$, and the last inequality from the minimization property that defines $\boldsymbol{x^{n+1}}$. For a given n, $\boldsymbol{x^{n+1}}$ is completely determined by $\boldsymbol{w^n}$; for $n = 0$, in particular, $\boldsymbol{x^1}$ is determined solely by $\boldsymbol{w^0}$, and independent of the choice of $\boldsymbol{x^0} \in \mathcal{J}(\boldsymbol{x})$. Next, we prove that the sequence $\{\Gamma_\nu^n\}_{n=1}^\infty$ is bounded as $||\boldsymbol{x^n}||_\nu^\nu \le \Gamma_\nu(\boldsymbol{x^1}, \boldsymbol{w^0}, \Omega_\epsilon) := L$. First,

$$\begin{aligned}&2\left[\Gamma_\nu^n(\boldsymbol{x^n}, \boldsymbol{w^n}, \Omega_\epsilon^n) - \Gamma_\nu^{n+1}(\boldsymbol{x^{n+1}}, \boldsymbol{w^{n+1}}, \Omega_\epsilon^{n+1})\right] \\ &\ge 2\left[\Gamma_\nu^n(\boldsymbol{x^n}, \boldsymbol{w^n}, \Omega_\epsilon^n) - \Gamma_\nu^{n+1}(\boldsymbol{x^{n+1}}, \boldsymbol{w^n}, \Omega_\epsilon^n)\right] \\ &= \langle \boldsymbol{x^n}, \boldsymbol{x^n}\rangle_{\boldsymbol{w^n}} - \langle \boldsymbol{x^{n+1}}, \boldsymbol{x^{n+1}}\rangle_{\boldsymbol{w^n}} \\ &= \langle \boldsymbol{x^n} + \boldsymbol{x^{n+1}}, \boldsymbol{x^n} - \boldsymbol{x^{n+1}}\rangle_{\boldsymbol{w^n}} \\ &= \langle \boldsymbol{x^n} - \boldsymbol{x^{n+1}}, \boldsymbol{x^n} - \boldsymbol{x^{n+1}}\rangle_{\boldsymbol{w^n}} \\ &= \sum_{i=1}^N w_i^n (x_i^n - x_i^{n+1})^\nu \\ &= L^{-1}||\boldsymbol{x^n} - \boldsymbol{x^{n+1}}||_{l_\nu}^\nu;\end{aligned} \tag{26}$$

therefore, we obtain that the sequence $\{\Gamma_\nu^n\}_{n=1}^\infty$ is bounded as $||\boldsymbol{x^n}||_\nu^\nu \le \Gamma_\nu(\boldsymbol{x^n}, \boldsymbol{w^n}, \Omega_\epsilon^n)$, and $\sum_{n=1}^\infty ||\boldsymbol{x^{n+1}} - \boldsymbol{x^n}||_\nu^\nu \le 2L^\nu$. In particular, we have

$$\lim_{n\to\infty} ||\boldsymbol{x^{n+1}} - \boldsymbol{x^n}||_\nu^\nu = 0. \tag{27}$$

Thus, the convergence is proved. ■

Theorem 2 ensures that, under certain conditions, the sequence of solutions provided by the proposed algorithm converges to a fixed point as a local minima. According to [23], such local convergence results are common for nonconvex optimization problems, e.g., l_ν-norm minimization solving by IRLS, and are actually global solutions as shown numerically in [26].

2) Complexity: The computational complexity reduction of the proposed AR-IRLS algorithm comes from two parts. Firstly, the computational complexity reduction is contributed by the fewer number of iterations. In each iteration of the conventional IRLS algorithms, the complexity of matrix multiplication $\boldsymbol{\Phi W^{(l)} \Phi^t}$ is $O(NM^2)$ since matrix $\boldsymbol{W^{(l)}}$ is diagonal, and the inverse of $(\boldsymbol{\Phi W^{(l)} \Phi^t} + \lambda(\boldsymbol{x^{(l)}}) * \boldsymbol{I})$ takes $O(M^3)$. Therefore, the complexity of solving $(\boldsymbol{\Phi W^{(l)} \Phi^t} + \lambda(\boldsymbol{x^{(l)}}) * \boldsymbol{I})^{-1}$ is $O(NM^2)$ due to $N > M$. Secondly, the computational complexity reduction is contributed by the fewer compressive samples required to guarantee the reconstruction performance. In the proposed AR-IRLS algorithm, the minimum number of compressive samples M is reduced, which leads to a large computational complexity reduction as the complexity of solving $(\boldsymbol{\Phi W^{(l)} \Phi^t} + \lambda(\boldsymbol{x^{(l)}}) * \boldsymbol{I})^{-1}$ is $O(NM^2)$. The performance analyses of the reduced iterations and compressive samples are further shown in experimental results.

IV. Proposed Descent-Based Algorithm for Decision Threshold Setting

If the original signal is noise-free and the number of samples M is large enough, the threshold φ_d for decision making could be set as the magnitude of the smallest element in the reconstructed

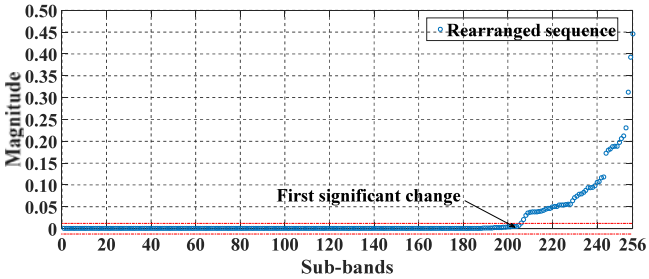

Fig. 2. The sorted sequences of the sub-bands and their first significant change.

signals, to ensure zero miss and low false alarms. However, in real-time processing, the reconstruction error increases as M is reduced, and it is further mixed with the noise whose variance is unknown and varying. Therefore, the traditional noise variance based methods for threshold setting as in (9) are not applicable anymore.

The rule of the proposed descent-based algorithm for φ_d setting is to locate the "first significant change" in the sorted sequence as illustrated by Fig. 2. Specifically, this algorithm first divides the reconstructed signal $\boldsymbol{x}^* \in \mathbb{R}^N$ into L sub-bands and therefore each sub-band contains $b = N/L$ elements. The average value of each sub-band is used to form the sequence:

$$\boldsymbol{p} = \{p_i\}_{i=1}^{L} \text{ where } p_i = E\left[\sum_{j=(b\cdot i+1)}^{b\cdot(i+1)} x_j^*\right] \tag{28}$$

Then we sort all elements of $\boldsymbol{p}$ in an ascending order in term of their magnitudes, which is donated by the sequence $\boldsymbol{p}^s = \{p_i^s\}_{i=1}^{L}$, i.e., p_1^s is the smallest element and p_L^s is the largest element in $\boldsymbol{p}$. Then we define the increment value between two adjacent elements in $\boldsymbol{p}^s$ by $\nabla p_i^s = (p_i^s + p_{i+1}^s)/2$. Since the original signal contains noise, which means that the reconstructed signal contains both the reconstruction error and noise, φ_d should be set equal to or slightly larger than the magnitude of the smallest element in the set of the largest $\tau\%$ elements so that the influence of the possible noise fluctuation could be diminished, where τ should be chosen to be large enough, such that the primary components in the signal $\boldsymbol{x}^*$ can not be missed.

The algorithm compares ∇p_i^s with the values from ∇p_1^s to ∇p_{i-1}^s. If p_i^s belongs to the largest $\tau\%$ part of $\boldsymbol{p}^s$ and ∇p_i^s is larger than ∇p_1^s to ∇p_{i-1}^s, we locate p_i^s as the "first significant change"; otherwise we increase i until the "first significant change" is obtained. We adopt this value as the threshold to distinguish the primary components and the combination of noise and reconstruction errors. It should be noted that the larger the sub-band, the simpler the algorithm becomes since less increment calculations and iterations are required. But the performance may be degraded if L is too small. The "first significant change" exists since in the reconstructed signal $\boldsymbol{x}^*$, the true nonzeros are large in magnitude and small in number, while the noise and false ones are large in number and small in magnitude due to the nature of the IRLS algorithm [5]. Therefore, the magnitudes of the true nonzeros are spread out, while those of the noise and reconstruction errors ones are clustered.

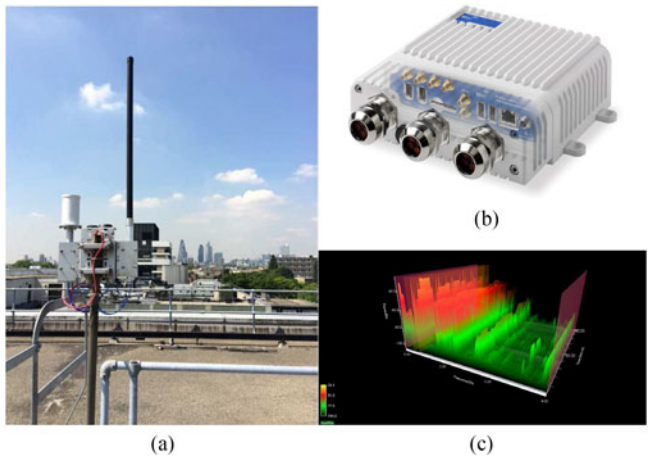

Fig. 3. (a) The outdoor antenna. (b) The RFeye node. (c) The captured power spectrum density at Queen Mary University of London.

V. Experimental Results

As a proof of concept for the proposed scheme, we discuss a series of experiments to test them using both simulated signals and real-world signals in this section.

A. Experiment Setups and Performance Measures

To verify the recovery accuracy of the proposed AR-IRLS algorithm that works with varying bandwidths and power levels in the primary signals, the simulated signals $\boldsymbol{x}_0^{\text{sim}}$ are generated by choosing k nonzero components uniformly at random out of $N = 1024$ and drawing the amplitude of each nonzero component from a uniform distribution of $U([-1, 1])$, where the sparsity level is $\mu = k/N$. The entries of the sensing matrix $\boldsymbol{\Phi} \in \mathbb{R}^{M\times N}$ are generated by an i.i.d. Gaussian process with zero mean and variance $1/M$, where M/N is the corresponding compressive ratio ρ.

The real-world TVWS signals $\boldsymbol{x}_0^{\text{real}}$ are received by an RFeye node, which is an intelligent spectrum monitoring system that can provide real-time 24/7 monitoring of the radio spectrum [47]. The RFeye node is located at Queen Mary University of London (51.523021° N 0.041592° W), and the antenna height is about 15 meters above ground, which is shown in Fig. 3. The frequency of the received real-world TVWS signal ranges from 470 to 790 MHz and the channel bandwidth is 8 MHz in Europe. The setting is consistent with the current bandwidth used in TV broadcasting. Therefore, the total bandwidth of the real-world signals is 320 MHz.

To quantify the reconstruction accuracy of the proposed algorithm, we calculate the conventional relative mean square error (r-MSE):

$$\text{r-MSE} = \frac{||\boldsymbol{x}^* - \boldsymbol{x}_0||}{||\boldsymbol{x}_0||}, \tag{29}$$

where $\boldsymbol{x}_0 = \boldsymbol{x}_0^{\text{sim}}$ in the simulation mode and $\boldsymbol{x}_0 = \boldsymbol{x}_0^{\text{real}}$ in the real-time mode. We also calculate the acceptable reconstruction frequencies, which is the fraction of successful reconstructions, defined as the case with r-MSE $\leq 10^{-2}$. The convergence speed

TABLE I
COMPARISON AMONG CONVENTIONAL IRLS ALGORITHMS AND THE PROPOSED AR-IRLS ALGORITHM

Algorithm	Compression Capability	Sparsity Tolerance	Computational Complexity
Reg-IRLS	high	high	high
Unreg-IRLS	medium	medium	medium
IRL1	low	low	low
AR-IRLS	high	high	low

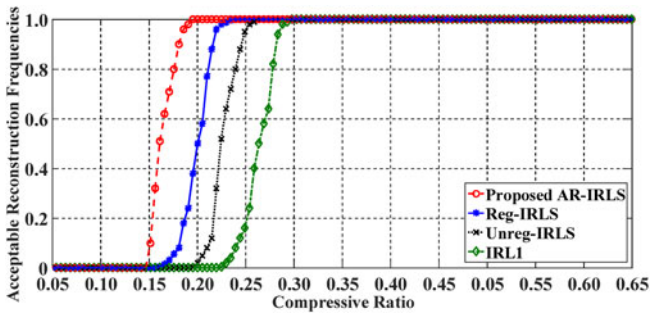

Fig. 4. Acceptable reconstruction frequencies vs. compressive ratio ρ between the proposed AR-IRLS algorithm and other conventional IRLS algorithms when sparsity level $\mu = 0.05$.

of the proposed AR-IRLS algorithm is also compared with the traditional regularized IRLS [26] (termed Reg-IRLS), unregularized IRLS (termed Unreg-IRLS), and the IRL1 approach [27] (termed IRL1). The comparison among these three conventional IRLS algorithms and the proposed algorithm is shown in Table I. The first two algorithms and the proposed AR-IRLS algorithm utilize the l_v-norm minimization, where v is set as 0.5, and the last one utilizes the l_1-norm minimization.

B. Results Over Simulated Signals

In this section, the acceptable reconstruction frequency performance of the proposed AR-IRLS algorithm is compared with the conventional IRLS algorithms including Reg-IRLS, Unreg-IRLS and IRL1. The impacts of system parameters such as the compression ratio and sparsity level are also investigated.

Fig. 4 shows the reconstruction performance against the compressive ratio ρ of the proposed AR-IRLS algorithm. For evaluation, we compare it with the other three IRLS algorithms. The sparsity level μ of the received signal is fixed to 0.05. It can be seen that the reconstruction performance of the proposed AR-IRLS algorithm is superior over that with the conventional IRLS algorithms under the same compression ratio. Therefore, a lower compressive ratio is enabled by the proposed AR-IRLS algorithm to achieve the same reconstruction accuracy, which decreases the required sampling rate in practical implementation.

As the PUs and SUs are frequently switching between the modes of offline and online, the sparsity levels of the received wideband signals in practice would fluctuate. A real-time wideband spectrum sensing scheme, therefore, should be robust against different signal sparsity levels. To validate that the proposed algorithm can work with different sparsity levels, Fig. 5 shows the reconstruction performance of the proposed scheme, which is improved with an increasing compressive ratio under different sparsity levels. Under the same sparsity level μ, the lower compressive ratio achieved by proposed sensing scheme in comparison with that of the conventional algorithms, could reduce the required sampling rate and lead to power savings. It is shown in Fig. 5 that the gap between adjacent curves gets smaller as the compressive ratio ρ increases, which matches the theoretical results regarding the formula $\rho = M/N \geq Ck\log(N/k)$ to calculate the minimum compressive ratio ρ for a Gaussian measurement matrix, where C denotes a constant and $k = \mu \cdot N$ [22].

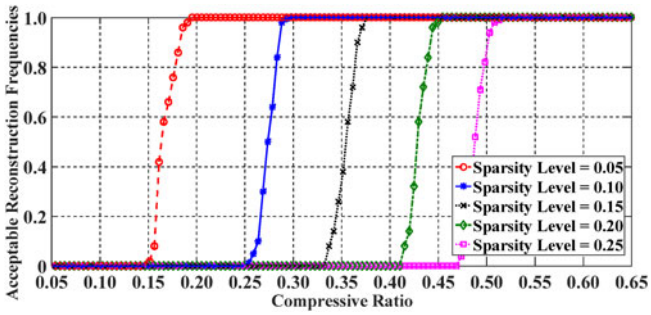

Fig. 5. Acceptable reconstruction frequencies vs. compressive ratio ρ for the proposed AR-IRLS algorithm under different sparsity levels $\mu = 0.05, 0.10, 0.15, 0.20, 0.25$.

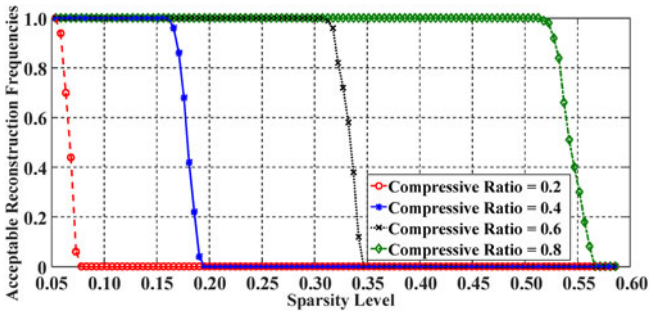

Fig. 6. Acceptable reconstruction frequencies vs. sparsity level μ under different compressive ratios $\rho = 0.2, 0.4, 0.6, 0.8$ for the proposed AR-IRLS algorithm.

To show the relationship between the reconstruction performance of the proposed algorithm and the sparsity level μ, we plot the acceptable reconstruction frequencies against the sparsity level μ ranging from 0.05 to 0.60 under compressive ratios $\rho = 0.2, 0.4, 0.6, 0.8$ in Fig. 6. It can be observed that the reconstruction performance degrades as the sparsity level increases, which indicates that more samples should be collected for signal reconstruction to ensure that the reconstruction performance is not degraded as μ increases. As Fig. 6 shows, although the signals with high sparsity levels require high compressive ratios, our algorithm can recover the signal with a sparsity level μ as high as 50%. By taking the advantage of robustness against different sparsity levels, our proposed scheme can deal with more SU on/off switchings over the spectrum of interest.

Fig. 7 shows the acceptable reconstruction frequency against the signal sparsity level μ under a compressive ratio $\rho = 0.8$

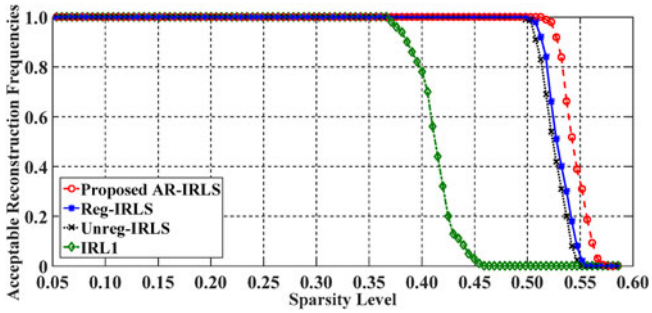

Fig. 7. Acceptable reconstruction frequencies vs. sparsity level μ between proposed AR-IRLS algorithm and other conventional IRLS algorithms when compressive ratio $\rho = 0.8$.

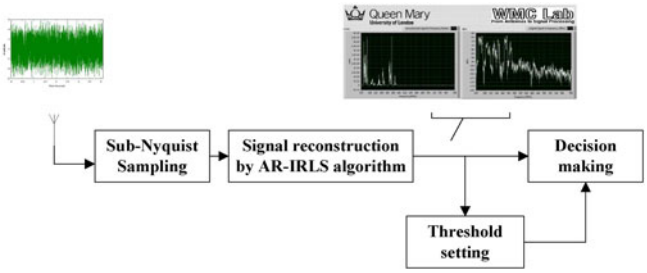

Fig. 8. Block diagram of the compressive spectrum sensing measurement for real-world signal on TVWS.

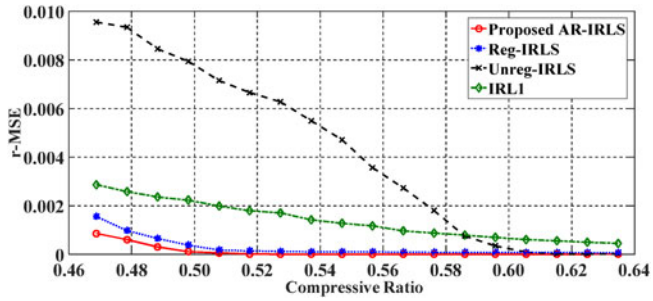

Fig. 9. r-MSE vs. compressive ratio ρ between proposed AR-IRLS algorithm and other conventional IRLS algorithms after 50 iterations.

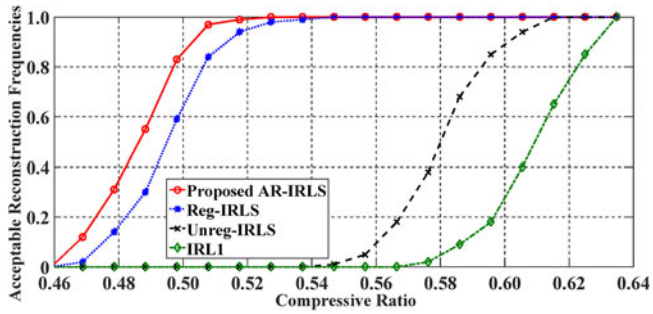

Fig. 10. Acceptable reconstruction frequencies vs. compressive ratio ρ between proposed AR-IRLS algorithm and other conventional IRLS algorithms after 50 iterations.

and the performance over a large sparsity level range could be observed in this setting. Although IRL1 has the minimum computational complexity, its reconstruction performance is the worst. The proposed one has the best reconstruction performance than the other three conventional IRLS algorithms, which recovers the largest sparsity range under the same ρ. This ensures that the proposed sensing scheme could cope with highly occupied channels.

C. Analysis on Real-world Signals

After the performance of the proposed scheme has been validated with the simulated signals, we further test it over real-world signals. The sparsity level of the received real-world signal is 0.2. The block diagram of the real-world signal measurement is shown in Fig. 8.

To analyze the reconstruction performance of the proposed scheme with real-world signals over the compressive ratio ρ, we compare the r-MSE of the proposed algorithm against the conventional algorithms under different compressive ratios. Fig. 9 shows that the reconstruction performance gets better with a higher compressive ratio at the receiver. More precisely, the relative reconstruction error, obtained after all algorithms converge, and averaged over enough repeats (e.g., 1000 runs), is depicted as a function of the compressive ratio ρ in Fig. 9. As shown in Fig. 9, we see that the proposed AR-IRLS algorithm only requires a few iterations to reach a satisfactory degree of accuracy and it outperforms the conventional algorithms. Fig. 10 indicates that as the compressive ratio ρ increases, better reconstruction performance is achieved. It is observed that the curve of Reg-IRLS is close to that of the proposed AR-IRLS

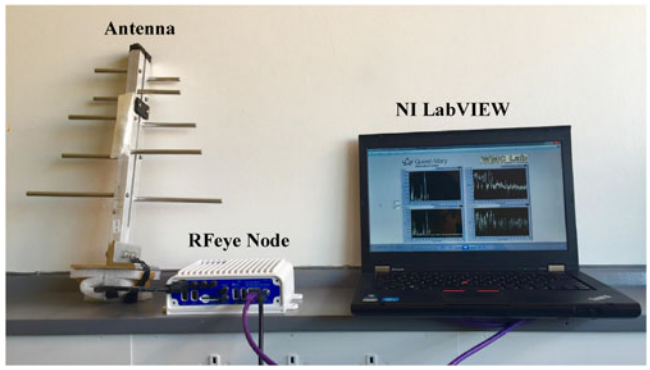

Fig. 11. Experimental setup for real-time processing and live compressive spectrum sensing testbed on TVWS.

since a small regularizer $\epsilon > 0$ is also added to the iteration process different from the other two. Fig. 10 also shows that the performance of the proposed IRLS-based spectrum sensing is better than that of the conventional IRLS-based spectrum sensing without regularization when the compression ratio is between 46% and 53%.

D. Real-Time Processing Measurement

After the performance of the proposed scheme is verified by both the simulated and real-world signals, it is further tested with real-time processing to demonstrate the improvement on iteration reduction. The experiment setup of real-time processing is shown in Fig. 11, which consists of the commercial directional UHF antenna, the RFeye node, and our real-time wideband

TABLE II
COMPARISON OF THE CONVERGENCE SPEED AND RECONSTRUCTION ACCURACY UNDER DIFFERENT SPARSITY LEVELS

k/N	Iterations		r-MSE after Convergence		Iterations Reduction
	Reg-IRLS	AR-IRLS	Reg-IRLS	AR-IRLS	
0.1	40	**12**	$7.8 \cdot 10^{-3}$	$\mathbf{6.1 \cdot 10^{-5}}$	70.0%
0.2	40	**14**	$7.2 \cdot 10^{-3}$	$\mathbf{4.3 \cdot 10^{-5}}$	65.0%
0.3	41	**17**	$8.7 \cdot 10^{-3}$	$\mathbf{8.8 \cdot 10^{-5}}$	58.6%
0.4	42	**20**	$9.6 \cdot 10^{-3}$	$\mathbf{6.3 \cdot 10^{-5}}$	52.4%
0.5	44	**26**	$1.1 \cdot 10^{-2}$	$\mathbf{8.6 \cdot 10^{-5}}$	41.0%

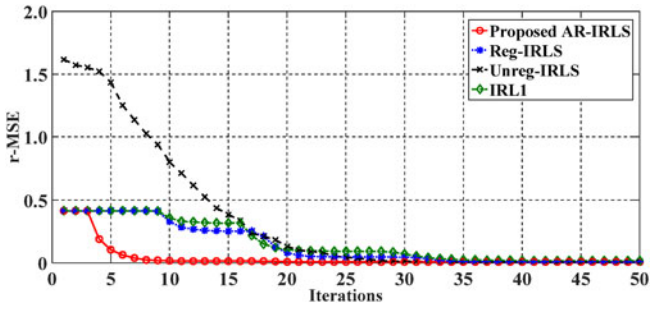

Fig. 12. r-MSE vs. Iterations between proposed AR-IRLS algorithm and other conventional IRLS algorithms when compressive ratio $\rho = 0.52$.

compressive spectrum sensing testbed that is developed over the NI LabVIEW software [48].

Table II shows the least number of iterations required by the proposed AR-IRLS algorithm and by the conventional Reg-IRLS algorithm to achieve a successful reconstruction, and their r-MSEs after the convergence under different sparsity levels μ. As seen from Table II, compared with the Reg-IRLS algorithm, the proposed AR-IRLS algorithm achieves faster convergence as it significantly reduces the number of required iterations for accurate reconstruction. For instance, the least number of iterations for successful reconstruction of the proposed AR-IRLS algorithm is reduced by up to 70% when the sparsity level $\mu = 0.1$, and 41% when the sparsity level $\mu = 0.5$. Furthermore, it shows that the proposed AR-IRLS algorithm achieves higher reconstruction accuracy than that of the Reg-IRLS algorithm under the same number of iterations. When the algorithms reach convergence, the r-MSE of the proposed algorithm is of order 10^{-5}, smaller than that of the proposed algorithm of order 10^{-3}. Therefore, the proposed AR-IRLS algorithm can achieve faster recovery with higher reconstruction resolution compared with the conventional IRLS algorithms.

Under a compression ratio of 0.64, we then compute the r-MSE of the proposed AR-IRLS algorithm against the number of iterations to evaluate its convergence speed and compare it with the conventional IRLS algorithms, to illustrate its reduction of required iterations under the same reconstruction accuracy, which is presented in Fig. 12. As the proposed algorithm directly converges to the actual global minimum shown in Theorem 2, it accomplishes the convergence with a faster speed, while other IRLS algorithms get into several wrong local solutions in the middle of the iteration processes. Moreover, since the proposed algorithm can converge to the actual global minimum without being stuck in wrong local solutions, the reconstruction accuracy of proposed algorithm is monotonically improving with the number of iterations.

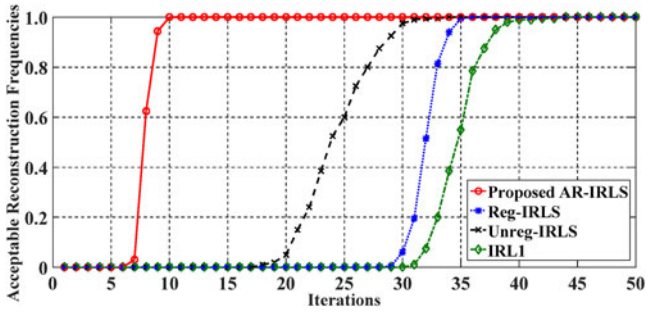

Fig. 13. Acceptable reconstruction frequencies vs. iterations between proposed AR-IRLS algorithm and conventional IRLS algorithms when compressive ratio $\rho = 0.52$.

Fig. 13 shows that the proposed algorithm achieves a 100% successful reconstruction frequency when the number of iterations increases to 9. In contrast, the conventional IRLS algorithms require at least 34 iterations to achieve the same performance. Therefore, the number of iterations is reduced by 70% in the proposed AR-IRLS algorithm without degrading the reconstruction accuracy. This gained benefits can significantly speed up the reconstruction process and reduce the computational burden in comparison with the conventional IRLS algorithms.

VI. CONCLUSION

In this paper, a real-time wideband spectrum sensing scheme with sub-Nyquist sampling was developed. To achieve fast reconstruction from the compressive samples, an adaptively-regularized iterative reweighted least squares (AR-IRLS) algorithm has been proposed to implement the CS-based wideband spectrum sensing with a high fidelity guarantee, which could cope with varying bandwidths and power levels in real-world signals. The proposed algorithm was tested over the real-world measurements after having been validated by the simulated signals with random supports and amplitudes. Numerical results showed that the convergence speed of the proposed reconstruction algorithm has been increased by up to 70% in comparison with the conventional iterative reweighted least squares (IRLS) algorithms, with 100x higher reconstruction accuracy, which makes the proposed AR-IRLS algorithm more efficient in real-time processing scenarios over shared spectrums such as TV white space (TVWS). Due to the optimization-based algorithm nature, the proposed AR-IRLS algorithm does have higher computational complexity than those greedy methods, e.g., orthogonal matching pursuit (OMP) and matching pursuit (MP) even though the proposed algorithm has reduced the number of iterations by up to 70% in comparison with the conventional IRLS algorithms.

Moreover, a descent-based algorithm has been proposed to distinguish the primary signals from the mixture of reconstruction errors and unknown noises, by dynamically setting the

threshold without any prior knowledge of the noise power. These benefits enable the proposed algorithm to be implementable for in real-time processing in new wireless services such as machine-to-machine communications. Consequently, the proposed algorithm would be a strong candidate to sense over a much wider spectrum spanning the cellular and ISM bands.

REFERENCES

[1] Office of Communications, "Digital dividend: Cognitive access," Jul. 2009. [Online]. Available: http://stakeholders.ofcom.org.uk/binaries/consultations/cognitive/statement/statement.pdf

[2] P. Kolodzy and I. Avoidance, "Spectrum policy task force," *Federal Commun. Comm., Washington, DC, Rep. ET Docket*, vol. 40, no. 4, pp. 147–158, 2002.

[3] F. Paisana, N. Marchetti, and L. A. DaSilva, "Radar, TV and cellular bands: Which spectrum access techniques for which bands?" *IEEE Commun. Surveys Tut.*, vol. 16, no. 3, pp. 1193–1220, Aug. 2014.

[4] O. Holland *et al.*, "To white space or not to white space: That is the trial within the ofcom TV white spaces pilot," in *Proc. IEEE Int. Conf. Dynamic Spectrum Access Netw.*, Stockholm, Sep. 2015, pp. 11–22.

[5] Z. Qin, Y. Gao, and C. G. Parini, "Data-assisted low complexity compressive spectrum sensing on real-time signals under sub-Nyquist rate," *IEEE Trans. Wireless Commun.*, vol. 15, no. 2, pp. 1174–1185, Feb. 2016.

[6] Z. Quan, S. Cui, A. H. Sayed, and H. V. Poor, "Optimal multiband joint detection for spectrum sensing in cognitive radio networks," *IEEE Trans. Signal Process.*, vol. 57, no. 3, pp. 1128–1140, Mar. 2009.

[7] H. Sun, A. Nallanathan, S. Cui, and C.-X. Wang, "Cooperative wideband spectrum sensing over fading channels," *IEEE Trans. Veh. Technol.*, vol. 65, no. 3, pp. 1382–1394, Mar. 2016.

[8] H. Sun, A. Nallanathan, C.-X. Wang, and Y. Chen, "Wideband spectrum sensing for cognitive radio network: A survey," *IEEE Trans. Wireless Commun.*, vol. 20, no. 2, pp. 74–81, Apr. 2013.

[9] Z. Zhang, Y. Xu, J. Yang, X. Li, and D. Zhang, "A survey of sparse representation: Algorithms and applications," *IEEE Access*, vol. 3, no. 7, pp. 490–530, May 2015.

[10] J. J. Meng, W. Yin, H. Li, E. Hossain, and Z. Han, "Collaborative spectrum sensing from sparse observations in cognitive radio networks," *IEEE J. Sel. Areas Commun.*, vol. 29, no. 2, pp. 327–337, Jan. 2011.

[11] W. Chen and I. J. Wassell, "A decentralized Bayesian algorithm for distributed compressive sensing in networked sensing systems," *IEEE Trans. Wireless Commun.*, vol. 15, no. 2, pp. 1282–1292, Feb. 2016.

[12] W. Chen, D. Wipf, Y. Wang, Y. Liu, and I. J. Wassell, "Simultaneous Bayesian sparse approximation with structured sparse models," *IEEE Trans. Signal Process.*, vol. 64, no. 23, pp. 6145–6159, Dec. 2016.

[13] Y. L. Polo, Y. Wang, A. Pandharipande, and G. Leus, "Compressive wideband spectrum sensing," in *Proc. IEEE Int. Conf. Acoust., Speech, Signal Process.*, Taipei, Apr. 2009, pp. 2337–2340.

[14] D. D. Arianandа and G. Leus, "Compressive wideband power spectrum estimation," *IEEE Trans. Signal Process.*, vol. 60, no. 9, pp. 4775–4789, Sep. 2012.

[15] G. Leus and D. D. Arianandа, "Power spectrum blind sampling," *IEEE Signal Process. Lett.*, vol. 18, no. 8, pp. 443–446, Aug. 2011.

[16] M. Mishali and Y. C. Eldar, "Blind multiband signal reconstruction: Compressed sensing for analog signals," *IEEE Trans. Signal Process.*, vol. 57, no. 3, pp. 993–1009, Mar. 2009.

[17] Y. Ma, Y. Gao, Y.-C. Liang, and S. Cui, "Reliable and efficient sub-Nyquist wideband spectrum sensing in cooperative cognitive radio networks," *IEEE J. Sel. Areas Commun.*, vol. 34, no. 10, pp. 2750–2762, Oct. 2016.

[18] T. Xiong, H. Li, P. Qi, Z. Li, and S. Zheng, "Pre-decision for wideband spectrum sensing with sub-Nyquist sampling," *IEEE Trans. Veh. Technol.*, vol. 66, no. 8, pp. 6908–6920, Aug. 2017.

[19] P. Feng and Y. Bresler, "Spectrum-blind minimum-rate sampling and reconstruction of multiband signals," in *Proc. IEEE Int. Conf. Acoust., Speech, Signal Process.*, vol. 3, Atlanta, GA, May 1996, pp. 1688–1691.

[20] Office of Communications, "Programme making and special events (PMSE)," Feb. 2015. [Online]. Available: https://www.ofcom.org.uk/manage-your-licence/radiocommunication-licences/pmse/

[21] J. A. Tropp and S. J. Wright, "Computational methods for sparse solution of linear inverse problems," *Proc. IEEE*, vol. 98, no. 6, pp. 948–958, Apr. 2010.

[22] D. L. Donoho, "Compressed sensing," *IEEE Trans. Inf. Theory*, vol. 52, no. 4, pp. 1289–1306, Apr. 2006.

[23] I. Daubechies, R. DeVore, and M. Fornasier, "Iteratively reweighted least squares minimization for sparse recovery," *Commun. Pure Appl. Math.*, vol. 63, no. 1, pp. 1–38, Jan. 2010.

[24] M. Wang, W. Xu, and A. Tang, "On the performance of sparse recovery via l_p-minimization," *IEEE Trans. Inf. Theory*, vol. 57, no. 11, pp. 7255–7278, Nov. 2011.

[25] D. L. Donoho, M. Elad, and V. N. Temlyakov, "Stable recovery of sparse overcomplete representations in the presence of noise," *IEEE Trans. Inf. Theory*, vol. 52, no. 1, pp. 6–18, Jan. 2006.

[26] R. Chartrand and V. Staneva, "Restricted isometry properties and nonconvex compressive sensing," *Inverse Problems*, vol. 24, May 2008, Art. no. 035020.

[27] E. J. Candes, M. B. Wakin, and S. P. Boyd, "Enhancing sparsity by reweighted l_1 minimization," *J. Fourier Anal. Appl.*, vol. 14, no. 5/6, pp. 877–905, Oct. 2008.

[28] J. Salt and H. Nguyen, "Performance prediction for energy detection of unknown signals," *IEEE Trans. Veh. Technol.*, vol. 57, no. 6, pp. 3900–3904, Nov. 2008.

[29] S. Atapattu, C. Tellambura, H. Jiang, and N. Rajatheva, "Unified analysis of low-SNR energy detection and threshold selection," *IEEE Trans. Veh. Technol.*, vol. 64, no. 11, pp. 5006–5019, Nov. 2015.

[30] N. Wang, Y. Gao, and X. Zhang, "Adaptive spectrum sensing algorithm under different primary user utilizations," *IEEE Commun. Lett.*, vol. 17, no. 9, pp. 1838–1841, Sep. 2013.

[31] S. Yoon, L. E. Li, S. C. Liew, R. R. Choudhury, I. Rhee, and K. Tan, "Quicksense: Fast and energy-efficient channel sensing for dynamic spectrum access networks," in *Proc. IEEE Int. Conf. Comput. Commun.*, Turin, Apr. 2013, pp. 2247–2255.

[32] Z. Qin, Y. Gao, M. Plumbley, and C. Parini, "Wideband spectrum sensing on real-time signals at sub-Nyquist sampling rates in single and cooperative multiple nodes," *IEEE Trans. Signal Process.*, vol. 64, no. 12, pp. 3106–3117, Jun. 2016.

[33] X. Zhang, Y. Zhang, Y. Ma, and Y. Gao, "RealSense: Real-time compressive spectrum sensing testbed over TV white space," in *Proc. IEEE Int. Conf. World Wireless, Mobile Multimedia Netw.*, Jun. 2017, pp. 1–3.

[34] Y. Ma, Y. Gao, A. Cavallaro, C. G. Parini, W. Zhang, and Y.-C. Liang, "Sparsity independent sub-Nyquist rate wideband spectrum sensing on real-time TV white space," *IEEE Trans. Veh. Technol.*, vol. 66, no. 10, pp. 8784–8794, Apr. 2017.

[35] D. L. Donoho, "For most large underdetermined systems of linear equations the minimal l_1-norm solution is also the sparsest solution," *Commun. Pure Appl. Math.*, vol. 59, no. 6, pp. 797–829, Mar. 2006.

[36] E. J. Candes and T. Tao, "Near-optimal signal recovery from random projections: Universal encoding strategies?" *IEEE Trans. Inf. Theory*, vol. 52, no. 12, pp. 5406–5425, Mar. 2006.

[37] Z. Lu, "Iterative reweighted minimization methods for l_p regularized unconstrained nonlinear programming," *Math. Programm.*, vol. 147, no. 1/2, pp. 277–307, Aug. 2014.

[38] Z. Ye, G. Memik, and J. Grosspietsch, "Energy detection using estimated noise variance for spectrum sensing in cognitive radio networks," in *Proc. IEEE Wireless Commun. Netw. Conf.*, Las Vegas, NV, Mar. 2008, pp. 711–716.

[39] Z. Xu, X. Chang, F. Xu, and H. Zhang, "$l_{1/2}$ regularization: A thresholding representation theory and a fast solver," *IEEE Trans. Neural Netw. Learn. Syst.*, vol. 23, no. 7, pp. 1013–1027, Jul. 2012.

[40] X. Zhou, R. Molina, F. Zhou, and A. K. Katsaggelos, "Fast iteratively reweighted least squares for l_p regularized image deconvolution and reconstruction," in *Proc. IEEE Int. Conf. Image Process.*, Paris, Oct. 2014, pp. 1783–1787.

[41] J. Yang, J. Wright, T. S. Huang, and Y. Ma, "Image super-resolution via sparse representation," *IEEE Trans. Image Process.*, vol. 19, no. 11, pp. 2861–2873, Nov. 2010.

[42] R. M. Mersereau and S. J. Reeves, "Optimal estimation of the regularization parameter and stabilizing functional for regularized image restoration," *Opt. Eng.*, vol. 29, no. 5, pp. 446–454, May 1990.

[43] N. P. Galatsanos and A. K. Katsaggelos, "Methods for choosing the regularization parameter and estimating the noise variance in image restoration and their relation," *IEEE Trans. Image Process.*, vol. 1, no. 3, pp. 322–336, Jul. 1992.

[44] F. Cao, M. Cai, Y. Tan, and J. Zhao, "Image super-resolution via adaptive l_p $(0 < p < 1)$ regularization and sparse representation," *IEEE Trans. Neural Networks. Learn. Syst.*, vol. 27, no. 7, pp. 1550–1561, Jul. 2016.

[45] X. Zhang, Y. Ma, and Y. Gao, "Adaptively regularized compressive spectrum sensing from real-time signals to real-time processing," in *Proc. IEEE Global Commun. Conf.*, Washington, DC, Dec. 2016.
[46] M. G. Kang and A. K. Katsaggelos, "General choice of the regularization functional in regularized image restoration," *IEEE Trans. Image Process.*, vol. 4, no. 5, pp. 594–602, May 1995.
[47] CRFS, "RFeye node," Oct. 2015. [Online]. Available: https://uk.crfs.com/zh-hans/products/rfeyenode/node-20-6/
[48] National Instruments, "LabVIEW system design software," Oct. 2016. [Online]. Available: http://www.ni.com/labview/

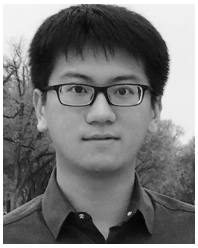

Xingjian Zhang (S'16) received double B.Sc. degrees (Hons.) in telecommunications engineering from Beijing University of Posts and Telecommunications, Beijing, China, and Queen Mary University of London, London, U.K., in 2014. He is currently working toward the Ph.D. degree in the School of Electronic Engineering and Computer Science, Queen Mary University of London, since 2014. His current research interests include cooperative wireless sensor networks, compressive sensing, real-time spectrum monitoring and analysis, and Internet of things (IoT) applications.

Yuan Ma (S'15–M'17) received the B.Sc. degree (Hons.) in telecommunications engineering from Beijing University of Posts and Telecommunications, Beijing, China, and the B.Sc. degree (Hons.) from Queen Mary University of London, London, U.K., in 2013, where she is currently pursuing the Ph.D. degree with the School of Electronic Engineering and Computer Science. Her current research interests include cognitive and cooperative wireless networking, sub-Nyquist signal processing, and spectrum analysis, detection, and sharing over TV white space.

Yue Gao (S'03–M'07–SM'13) received the Ph.D. degree from Queen Mary University of London (QMUL), London, U.K., in 2007. He was a Research Assistant, Lecturer (Assistant Professor), and Senior Lecturer (Associate Professor) at QMUL. He is currently a Reader in antennas and signal processing, and the Director of Whitespace Machine Communication Lab, School of Electronic Engineering and Computer Science, Queen Mary University of London (QMUL), London, U.K.. He is currently leading a team developing theoretical research into practice in the interdisciplinary area among smart antennas, signal processing, spectrum sharing, and Internet of things (IoT) applications. He has published more than 120 peer-reviewed journal and conference papers, 2 patents, and 2 book chapters. He is a co-recipient of the EU Horizon Prize Award on Collaborative Spectrum Sharing in 2016, and Research Performance Award from Faulty of Science and Engineering at QMUL in 2017.

He is an Editor for the IEEE TRANSACTIONS ON VEHICULAR TECHNOLOGY, the IEEE WIRELESS COMMUNICATION LETTER, and *China Communications*. He is currently the Cognitive Radio Symposium Co-Chair of the IEEE GLOBECOM 2017. He was the Signal Processing for Communications Symposium Co-Chair for IEEE ICCC 2016, the Publicity Co-Chair for IEEE GLOBECOM 2016, and the General Chair of the IEEE WoWMoM and iWEM 2017. He is a Secretary of the IEEE Technical Committee on Cognitive Networks and an IEEE Distinguished Lecturer of Vehicular Technology Society.

Shuguang Cui (S'99–M'05–SM'12–F'14) received the Ph.D degree in electrical engineering from Stanford University, Stanford, CA, USA, in 2005. Afterwards, he has been working as an Assistant, Associate, and Full Professor of electrical and computer engineering at the University of Arizona and Texas A&M University. He is currently a Child Family Endowed Chair Professor in Electrical and Computer Engineering at the University of California-Davis, Davis, CA, USA. His current research interests focus on data driven large-scale system control and resource management, large data set analysis, IoT system design, energy harvesting based communication system design, and cognitive network optimization. He was selected as the Thomson Reuters Highly Cited Researcher and listed in the Worlds' Most Influential Scientific Minds by ScienceWatch in 2014. He was the recipient of the IEEE Signal Processing Society 2012 Best Paper Award. He has served as the General Co-Chair and TPC Co-Chairs for many IEEE conferences. He has also been serving as the Area Editor for the IEEE SIGNAL PROCESSING MAGAZINE, and Associate Editor for the IEEE TRANSACTIONS ON BIG DATA, the IEEE TRANSACTIONS ON SIGNAL PROCESSING, IEEE JOURNAL ON SELECTED AREAS IN COMMUNICATIONS SERIES ON GREEN COMMUNICATIONS AND NETWORKING, and the IEEE TRANSACTIONS ON WIRELESS COMMUNICATIONS. He has been the elected member for IEEE Signal Processing Society SPCOM Technical Committee (2009–2014) and the elected Chair for IEEE ComSoc Wireless Technical Committee (2017–2018). He is a member of the Steering Committee for both the IEEE TRANSACTIONS ON BIG DATA and the IEEE TRANSACTIONS ON COGNITIVE COMMUNICATIONS AND NETWORKING. He is also a member of the IEEE ComSoc Emerging Technology Committee. He was elected as an IEEE Fellow in 2013 and an IEEE ComSoc Distinguished Lecturer in 2014.